be the natural linewidth.

An upper limit on narrowing due to diffusion broadening can be inferred from our general expression

$$\sigma_a(\omega)=\frac{\sigma_0\Gamma}{2\beta S}A\left(1+\frac{\alpha}{s+1}+\frac{\alpha^2}{(s+1)(s+2)}+\cdots\right).$$

When $\alpha\to\infty$, $\beta\to 0$, the above goes over to

$$\sigma_a(\omega)=\frac{\sigma_0\Gamma A}{2\beta S}\left(1+\frac{\alpha}{s}+\frac{\alpha^2}{s^2}+\cdots\right)$$

$$=\frac{\sigma_0\Gamma A}{2}\frac{1}{\Gamma+i\omega},$$

giving a Lorentzian with natural linewidth. This is the adiabatic approximation. In the present model which we have considered, namely, the Langevin model of diffusion, the satisfaction of the space-resolution condition does not yield any additional information regarding the time aspects of the motion; but if we can consider the atomic motion in a liquid where such a condition is satisfied, then γ-ray scattering can yield information regarding the dynamics of motion in the liquid.

*Presently visiting scientist at the National Physical Laboratory, New Delhi, India.

[1]K. S. Singwi and A. Sjölander, Phys. Rev. 120, 1093 (1960).

[2]A. J. F. Boyle, D. St. P. Bunbury, C. Edwards, and H. E. Hall, Proc. Phys. Soc. (London) 77, 129 (1961).

[3]P. P. Craig and N. Sutin, Phys. Rev. Letters 11, 460 (1963).

[4]T. Bonchev *et al.*, Zh. Eksperim. i Teor. Fiz. 50, 62 (1966) [Soviet Phys. JETP 23, 42 (1966)].

[5]S. L. Kordyuk *et al.*, Zh. Eksperim. i Teor. Fiz. 52, 611 (1967) [Soviet Phys. JETP 25, 400 (1967)].

[6]D. C. Champeney and F. W. D. Woodhams, J. Phys. B2, 620 (1968).

[7]S. Chandrasekhar, Rev. Mod. Phys. 15, 1 (1943).

[8]*Higher Transcendental Functions*, edited by A. Erdelyi (McGraw-Hill, New York, 1953), Vol. I, p. 255.

[9]K. S. Singwi and A. Sjölander, Phys. Rev. 119, 863 (1960).

[10]J. G. Dash and R. H. Nussbaum, Phys. Rev. Letters 16, 567 (1966).

PHYSICAL REVIEW B VOLUME 3, NUMBER 3 1 FEBRUARY 1971

Mössbauer Determination of Fe^{57} Nuclear Quadrupole Coupling Parameters in Ferric Oxychloride

R. W. Grant, H. Wiedersich, R. M. Housley, and G. P. Espinosa
Science Center, North American Rockwell Corporation, Thousand Oaks, California 91360

and

J. O. Artman
Departments of Electrical Engineering and Physics and Mellon Institute, Carnegie-Mellon University, Pittsburgh, Pennsylvania 15213

(Received 19 October 1970)

The nuclear quadrupole coupling parameters have been determined at the nonaxially symmetric Fe^{3+} site in ferric oxychloride by Mössbauer spectroscopic measurements. This compound should be suitable for checking theoretical models used to calculate electric field components and their derivatives in ionic solids. The quadrupole splitting (peak separation) is found to be 0.916 ± 0.001 mm/sec. The x, y, and z principal axes of the electric field gradient (EFG) are parallel to the c, b, and a crystallographic axes, respectively ($c<a<b$). The EFG asymmetry parameter is $\eta=0.32\pm0.03$ and $V_{zz}<0$. A lattice-sum calculation of the EFG based on the self-consistent monopole-point dipole model can be made to fit the data by suitable adjustment of the anion polarizabilities; however, the necessary polarizabilities and the Fe^{57} quadrupole moment which is obtained do not seem entirely satisfactory.

I. INTRODUCTION

In recent years, the calculation of electric potentials and potential derivatives at sites in ionic crystals has usually employed some version of the self-consistent monopole-point dipole model.[1-5] Briefly, the model involves the evaluation of monopole contributions by a lattice-sum technique and the inclusion of dipole contributions by a self-consistent calculation of ionic dipole moments. The dipole-moment calculation requires independent knowledge of ionic polarizabilities.

There have been few experimental tests of this model. The most rigorous of these was a compari-

son of calculated and experimental electric field-gradient (EFG) tensors for the two Al and one Be nuclear sites in the mineral chrysoberyl[5]; results were ambiguous. By allowing the oxygen polarizability to be an adjustable parameter, reasonable agreement could be obtained with most of the data. However, the required oxygen polarizability of ≈ 1 Å^3 is less than half the value determined from careful analysis of optical data for BeO.[4]

Electron charge distributions in crystals as determined from x-ray data suggest that multipole expansions to represent electric potentials probably should contain terms of higher order than monopole and dipole. Calculations of the quadrupole contributions to the EFG tensor at the Fe nuclei in Fe_2O_3 also suggest that quadrupole contributions will not generally be negligible.[6]

It has recently been pointed out[7,8] that significant contributions to the EFG at the nucleus can be caused by distortion of closed-shell wave functions owing to overlap with occupied orbitals on near-neighbor atoms. While explicit calculations have so far only been reported for Al^{3+} in Al_2O_3 and Fe^{3+} in Fe_2O_3, the effect is probably more general.

Thus, it seems desirable to obtain more data suitable for checking model calculations. Flinn[9] has suggested FeOCl as a compound well suited for this purpose. Two independent quadrupole coupling parameters can be evaluated for both the Fe^{3+} and Cl^- sites giving a total of four independent quantities. Eliminating the quadrupole moment of Fe^{57} which is not too well known still leaves three independent quantities.

In the present paper, Mössbauer data fixing the quadrupole coupling parameters at the Fe^{3+} site are presented. The possible interpretation of the data in terms of the self-consistent monopole-point model is discussed.

II. EXPERIMENTAL

Mössbauer spectra were obtained with an automated mechanical constant-velocity spectrometer operating in the normal transmission mode; the spectrometer is described briefly elsewhere.[10] Two sources of resonant Fe^{57} 14.4-keV radiation were used: Co^{57} in Cu and Co^{57} in α-Fe. Both sources and the single-crystal FeOCl absorber were kept at room temperature (23 ± 1 °C).

Crystals of FeOCl were prepared by vapor-phase reaction; a similar procedure was reported previously.[11] Amounts of Fe_2O_3 and $FeCl_3$ appropriate to make 0.1 mole of FeOCl were sealed in an evacuated fused silica cylinder (3-in. diam × 6 in. long) and heated for one week at 450 °C. Thermal gradients present in the furnace cause crystals of FeOCl to grow on the coolest part of the glass tube. The dark-red crystals have a thin bladelike habit with the crystallographic b axis ($c < a < b$) perpendicular to the platelet and the c axis parallel to the longest platelet dimension.

A single crystal of sufficient size ($2 \times 4 \times 0.01$ mm) to be useful as an absorber was carefully selected. The crystal surface density, determined by weighing the crystal on a microbalance and measuring the surface area with the aid of photographic enlargement, was found to be 3.51 ± 0.01 mg/cm^2. Microscopic examination of the crystal indicated a uniform thickness to within the observational accuracy ($\approx 10\%$); because the absorber was very thin, uncertainty in data corrections caused by a nonuniform absorber thickness was negligible.

The crystal was oriented to better than 0.5° by using Burger precession-camera x-ray-diffraction photography. The quality of the crystal was ascertained by observations of the Burger precession-camera diffraction patterns taken at different positions on the surface and by optical examination with polarized light.

All Mössbauer data were obtained with the γ-ray propagation direction $\vec{k}$ parallel to the crystallographic b axis. To avoid possible geometrical corrections to the data, a source-to-absorber distance was chosen so that the maximum deviation of $\vec{k}$ from b was $< 4°$. All data were least-squares fit to two Lorentz line shapes with no constraints; the experimental linewidths varied between 0.25 and 0.26 mm/sec. Background corrections of $\approx 22\%$ were made by standard filter techniques.[12]

III. SYMMETRY CONSIDERATIONS

The crystal structure of FeOCl was first determined by Goldztaub[11,13] and recently refined by Lind.[14] Crystals of FeOCl belong to the orthorhombic space group $Pmnm$ (D_{2h}^{13}) with two FeOCl per unit cell; unit-cell dimensions are $a = 3.780$, $b = 7.917$, and $c = 3.302$ Å. All ions are on twofold special positions with point symmetry mm. The two Fe^{3+} ions are on positions b with coordinates $(0, y, \frac{1}{2}; \frac{1}{2}, \bar{y}, 0)$. A projection of three cis-$[FeCl_2O_4]^{-7}$ octahedra onto the ab plane is shown in Fig. 1. Ion positions are given in fractional units along c. The position of the twofold rotation and screw axes which relate the three sets of twofold sites per unit cell are indicated. The two mirror planes and diagonal glide plane are not shown but can easily be discerned from an inspection of the figure.

The EFG is described by a symmetric second-rank tensor. This tensor can be diagonalized in a principal axis system and completely specified by the diagonal elements (V_{xx}, V_{yy}, V_{zz}) and by the orientation parameters relating the principal axes (x, y, and z) to the crystal axes.[15] The diagonal elements are chosen as $|V_{zz}| \geq |V_{yy}| \geq |V_{xx}|$. Because the EFG is a traceless tensor, it is customary to define two independent parameters $q = V_{zz}/|e|$ and the asymmetry parameter $\eta = (V_{xx} - V_{yy})V_{zz}^{-1}$, where e

is the electronic charge. The choice of principal axes limits η to $0 \leq \eta \leq 1$.

The point symmetry *mm* of the Fe^{3+} site in FeOCl requires the principal axes of the EFG to be parallel to the *a*, *b*, and *c* crystallographic axes but places no restrictions on η. Since the EFG is symmetric with respect to inversion, the principal axes at both crystallographically equivalent Fe^{3+} sites per unit cell have identical orientations relative to the crystal axes; this considerably simplifies the data analysis.

In general, in all but extremely thin single crystals, both polarization and dispersion will affect Mössbauer measurements of relative absorption intensities. However if only one set of nonmagnetically ordered crystallographically equivalent Fe^{57} resonant sites exists in the unit cell, the index of refraction may be diagonalized for any $\vec{k}$ and dispersive effects can be neglected (a proof of this point is given in the Appendix). Thus, for any $\vec{k}$ in FeOCl at room temperature, only pure absorption effects need be considered in the data analysis.

IV. MÖSSBAUER RESULTS

The room-temperature Mössbauer parameters of FeOCl were determined by statistical analysis of 22 independent spectra. The averaged spectra and a least-squares fit to two Lorentz line shapes are shown in Fig. 2. The quadrupole splitting ΔE_Q and isomer shift δ observed in FeOCl at 23 °C (relative to the Co^{57}–Cu source) and corresponding error limits[16] are

$$\Delta E_Q = 0.916 \pm 0.001 \text{ mm/sec},$$

$$\delta = +0.165 \pm 0.001 \text{ mm/sec}.$$

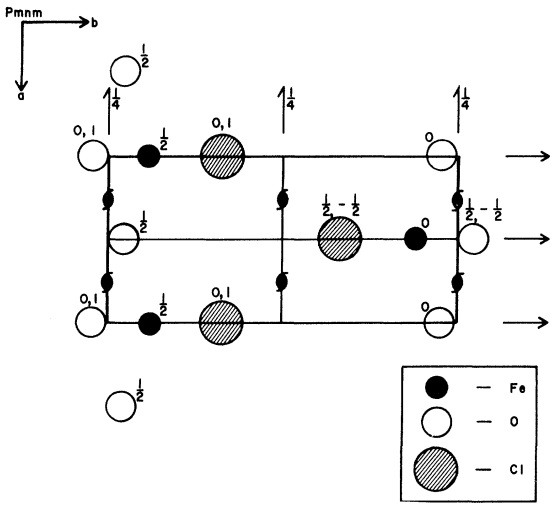

FIG. 1. Projection of three cis-$[FeCl_2O_4]^{-7}$ octahedra in FeOCl onto the *ab* plane. Ion positions are given in fractional units of *c* and positions of rotation axes are indicated. Data are from Ref. 14.

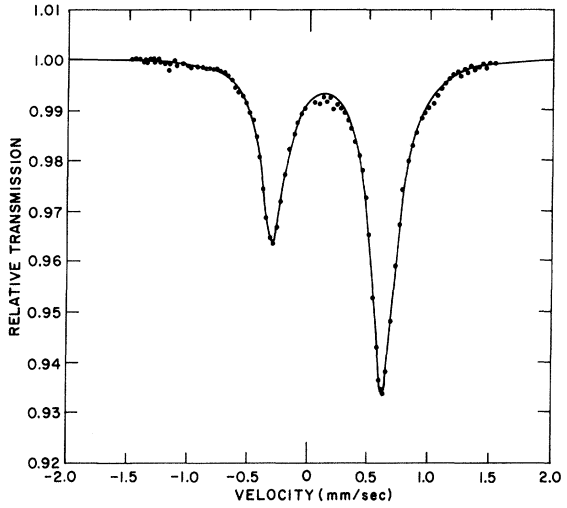

FIG. 2. Mössbauer spectrum obtained with a Co^{57} in Cu source and single-crystal FeOCl absorber ($\vec{k} \parallel b$). Source and absorber were at room temperature (23 °C).

For Fe^{57}, the energy difference between the two absorption lines of a pure quadrupole split doublet is

$$\Delta E_Q = \tfrac{1}{2} e^2 q Q (1 + \tfrac{1}{3}\eta^2)^{1/2}. \quad (1)$$

The isomer shift of the Co^{57}-Cu source relative to α-Fe (23 °C) is -0.222 ± 0.002 mm/sec.

The analysis of the EFG parameters was similar to a procedure used previously[10,17] and thus only a brief description will be given here. We define a dimensionless absorption area $A = 2A_{exp}/\pi f \Gamma$, where A_{exp} is the experimentally measured absorption area (after background correction), f is the recoil-free fraction of the Co^{57}-Cu source at 23 °C ($f = 0.71$)[18] and Γ (0.097135 mm/sec) is the natural linewidth of the 14.4-keV state.[19] The A values and ratio A_3/A_1 are given in Table I; subscripts 3 and 1 refer to the lower- and higher-energy absorption lines in the FeOCl spectrum, respectively. Because the crystal is thin and saturation effects therefore are small, the A_3/A_1 ratio indicates that $V_{zz} < 0$ and that $V_{yy} \parallel b$ (see Fig. 4, Ref. 20). The initial value of η estimated from these uncorrected data is 0.28. Saturation corrections were next applied to the data. For relatively thin absorbers as in the present case, a useful expression is developed in Ref. 17, Eq. (21), which for convenience is reproduced here:

$$p = A + \tfrac{1}{4}(1 + a^2)A^2 + \tfrac{1}{16}(1 + a^2 + 2a^4)A^3 + \tfrac{5}{384}(1 + a^4 + 6a^6)A^4 + \ldots, \quad (2)$$

where p is the dimensionless area after correction for saturation and polarization, and a is the fractional polarization of the absorption line. Expressions for calculating a with arbitrary EFG parameters and $\vec{k}$ are given in Ref. 17. Neglecting polarization of the absorption lines ($a = 0$) leads to the p_3^0/p_1^0 value

TABLE I. Experimental and corrected data for FeOCl at 23 °C and $\vec{k} \parallel b$.[a]

Sample thickness (mg/cm^2)	3.51 ±0.01
A_3	0.171 ±0.004
A_1	0.327 ±0.006
A_3/A_1	0.522 ±0.006
P_3^0/P_1^0	0.499 ±0.006
P_3	0.186 ±0.006
P_1	0.362 ±0.007
P_3/P_1	0.513 ±0.006
$f_b'(\alpha = 8.2)$	0.50 ±0.03

[a]Experimental uncertainties are 1 standard deviation of the mean value.

shown in Table I which is consistent with $\eta^0 = 0.36$. Polarization corrections were applied by calculating initial a values based on η^0 and iterating the above expression to convergence. The corrected p_3, p_1, and p_3/p_1 values are given in Table I. The value of η consistent with this p_3/p_1 ratio is $\eta = 0.32 \pm 0.03$.

To determine the orientation of V_{zz} in the absorber ac plane, a linearly polarized Co^{57} in α-Fe source (magnetized by a field of $\vec{H}_s \approx 0.5$ kOe in the α-Fe foil plane) was used in a manner similar to that employed earlier by Johnson *et al.*[21] Spectra obtained with this source and the single-crystal absorber oriented so that $\vec{H}_s \perp \vec{k}$, $\vec{k} \parallel b$ and $\vec{H}_s \parallel a$ and $\parallel c$ are shown in Figs. 3(a) and 3(b), respectively. The expected line positions of this source/absorber

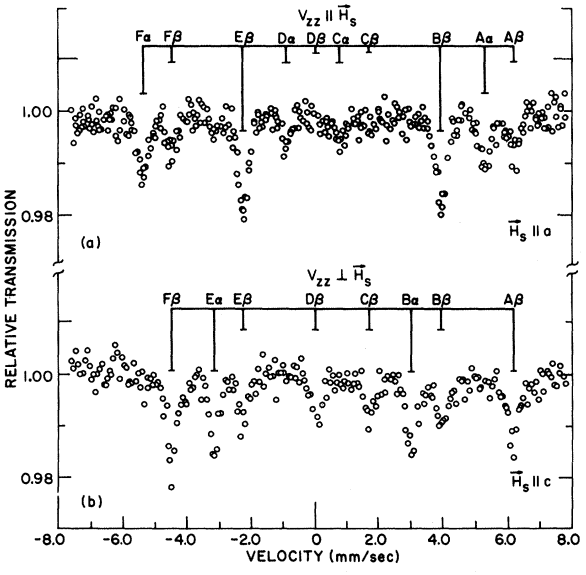

FIG. 3. Mössbauer spectra taken with a linearly polarized Co^{57} in α-Fe source (23 °C) and a single-crystal FeOCl absorber (23 °C). The experimental arrangement was $\vec{k} \parallel b$, $\vec{H}_s \perp \vec{k}$, and (a) $\vec{H}_s \parallel a$, (b) $\vec{H}_s \parallel c$. Expected line postitions and intensities (assuming $\eta = 0$) for $V_{zz} \parallel \vec{H}_s$ and $V_{zz} \perp \vec{H}_s$ are shown in (a) and (b), respectively.

combination are easily calculated by simply considering the overlap of the six emission lines with the two absorption lines. Because η is relatively small, existing expressions[22] (strictly valid only for $\eta = 0$) can be used to estimate the expected line intensities. Labeling emission lines by Roman characters and absorption lines by Greek characters in order of ascending energy, the expected line positions and intensities for the cases $V_{zz} \parallel \vec{H}_s$ and $V_{zz} \perp \vec{H}_s$ are indicated in Figs. 3(a) and 3(b), respectively. Comparison of these calculated spectra with the experimental data shows that V_{zz} is parallel to a; thus, V_{xx} is parallel to c. A summary of the experimentally determined EFG parameters observed at the Fe^{57} site in FeOCl at 23 °C is given in Table II.

The data in Table I can be used to calculate the recoil-free fraction parallel to b of the Fe^{57} ions, f_b'. We evaluated the expression $(p_1 + p_3)_b = n f_b' \sigma_0$, where n is the number of resonant nuclei per unit area and σ_0 is the fixed nucleus cross section. Symmetry considerations similar to those in Sec. III restrict the principal axes of the mean-square displacement tensor to be parallel to a, b, and c; thus, f_b' is the same at both Fe^{3+} sites in the unit cell. For an internal conversion coefficient of α equal to 8.2 ± 0.2,[23,24]

$$\sigma_0 = (1/2\pi)\lambda^2(1 + 2I_e)(1 + 2I_g)^{-1}(1 + \alpha)^{-1}$$
$$= 2.56 \times 10^{-18}\ \text{cm}^2.$$

Here I_e and I_g are the excited and ground-state nuclear spins, and λ is the wavelength of the 14.4125-keV radiation.[19] By use of the measured surface density of the FeOCl crystal, the Mössbauer result is $f_b' = 0.50 \pm 0.03$. The mean-square displacment parallel to b, $\langle r^2 \rangle_b$, is related to f_b' by $f_b' = e^{-k^2 \langle r^2 \rangle_b}$; for Fe^{57}, $k^2 = 5.334 \times 10^{17}\ \text{cm}^{-2}$. Because the x-ray structure refinement[14] included anisotropic thermal factors, a comparison of the f_b' values determined by both Mössbauer and x-ray-diffraction techniques can be made. The x-ray data lead to f_b' (x ray) = 0.54 ± 0.03 (this error limit which is three times the estimated standard error could be somewhat larger if possible systematic errors were considered). Thus, reasonably close agreement is obtained by the two techniques.

TABLE II. Room-temperature EFG parameters, at the Fe^{3+} site in FeOCl.[a]

ΔE_Q	= 0.916 ± 0.001 mm/sec
η	= 0.32 ±0.03
V_{zz}	< 0
V_{zz}	$\parallel a$
V_{yy}	$\parallel b$
V_{xx}	$\parallel c$

[a]Experimental uncertainties are 1 standard deviation of the mean value.

V. MODEL CALCULATIONS

We have calculated the EFG parameters predicted by the self-consistent monopole-point dipole model at all occupied crystal sites. A version of the symmetrized chargeless cluster method was used.[1,25] Atomic positions were based on the recent structure refinement of Lind.[14] Lattice sums were carried out over an ellipsoid with principal radii proportional to the unit-cell dimensions and corresponding in magnitude to five lattice constants; this ellipsoid was sufficiently large for convergence. The results are shown in Table III, where E_i is an electric field component and V_{ii} is one of the principal components of the EFG tensor; the superscript M denotes a monopole contribution while Fe, Cl, and O denote the contributions due to unit dipoles on the Fe^{3+}, Cl^-, and O^{2-} sites, respectively.

To assess the importance of geometrical uncertainties, calculations of the monopole EFG contributions were performed in which crystallographic parameters were varied several standard deviations. The change in EFG tensor elements was typically a few percent.

In terms of the model the experimentally determined quadrupole coupling parameters

$$U_{ii}^{\exp} = [V_{ii}Q(1-\gamma_\infty)/|e|]$$

directly derivable from the data in Table II are given by

$$U_{ii}^{\exp} = [Q(1-\gamma_\infty)/|e|](V_{ii}^M + V_{ii}^0 P_O + V_{ii}^{Cl} P_{Cl}), \quad (3)$$

where γ_∞ is the Sternheimer antishielding factor and P_O and P_{Cl} are the dipole moments on the O^{2-} and Cl^- sites, respectively. Cation polarizability is neglected. Only two of the three possible equations are independent.

TABLE III. Calculated field and field-gradient parameters in FeOCl.

	Units	At Fe^{3+} site	At O^{2-} site	At Cl^- site
$E_b^m/\|e\|$	Å^{-2}	−0.08185	0.17318	0.43785
$V_{aa}^m/\|e\|$	Å^{-3}	−0.30332	0.63630	−0.33676
$V_{bb}^m/\|e\|$	Å^{-3}	0.09002	−0.40855	0.18276
$V_{cc}^m/\|e\|$	Å^{-3}	0.21330	−0.22777	0.15400
E_b^{Fe}	Å^{-3}	−0.11895	−0.27181	−0.02765
V_{aa}^{Fe}	Å^{-4}	−0.07367	−0.24407	−0.11081
V_{bb}^{Fe}	Å^{-4}	0.11854	0.56545	−0.09914
V_{cc}^{Fe}	Å^{-4}	−0.04487	−0.32138	0.20996
E_b^O	Å^{-3}	−0.27181	0.07177	−0.07150
V_{aa}^O	Å^{-4}	0.56282	−0.12282	0.06816
V_{bb}^O	Å^{-4}	−0.06712	0.20304	−0.11117
V_{cc}^O	Å^{-4}	−0.49570	−0.08022	0.04301
E_b^{Cl}	Å^{-3}	−0.02765	−0.07150	−0.18171
V_{aa}^{Cl}	Å^{-4}	0.09771	−0.02414	0.02443
V_{bb}^{Cl}	Å^{-4}	0.10683	0.03518	−0.03801
V_{cc}^{Cl}	Å^{-4}	−0.20454	−0.01104	0.01358

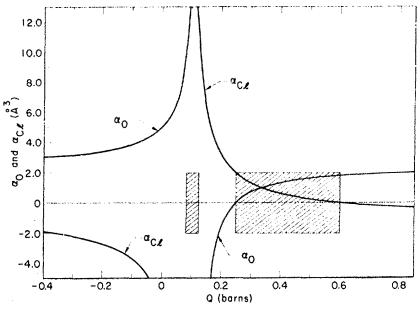

FIG. 4. Relation of O^{2-} and Cl^- polarizabilities to Q as predicted by self-consistent monopole-point dipole-model calculation. Expressions are given in Eq. (5) of text. Cross-hatched lines indicate possible solution ranges.

The dipole moments are given by

$$P_O = \alpha_O(E_O^M + E_O^O P_O + E_O^{Cl} P_{Cl}),$$
$$P_{Cl} = \alpha_{Cl}(E_{Cl}^M + E_{Cl}^O P_O + E_{Cl}^{Cl} P_{Cl}), \quad (4)$$

where α_o and α_{Cl} are the O^{2-} and Cl^- polarizabilities, respectively. Equations (3) and (4) can be rearranged to give expressions for α_O and α_{Cl} in terms of Q. Using the experimental results (converted to appropriate units) and $\gamma_\infty = -9.14$,[26] the expressions are the hyperbolas

$$\alpha_O = \frac{0.618Q - 0.154}{0.250Q - 0.0307}, \quad \alpha_{Cl} = \frac{-0.454Q + 0.274}{0.476Q - 0.0388}, \quad (5)$$

where Q is in barns (b) and α is in Å^3. A graph of these relations is shown in Fig. 4. Since negative α's are meaningless, it can be seen that only two restricted ranges of α's and Q give possible solutions. These ranges are indicated by cross-hatched lines on the figure.

VI. DISCUSSION

The first range of solutions has very large α values and can probably be discounted as physically unreasonable; however, the second range which contains $\alpha_{Cl} \approx \alpha_O \approx 1$ Å^3 and $Q \approx 0.33$ b is more significant. Data on Fe_2O_3 are also compatible with $\alpha_O \approx 1$ Å^3 and $Q \approx 0.33$ b; the best fit to the chrysoberyl data[5] was obtained with $\alpha_O \approx 1$ Å^3.

This limited agreement is probably not a good indication of the adequacy of the model. Unless α_O is strongly dependent on local ionic environment, a value of $\alpha_O = 1$ Å^3 seems unreasonable when compared to the value 2.19 Å^3 obtained by careful analysis of optical data in BeO.[4] Possible sources of difficulty with the presently employed model are evident. Covalency, overlap, and higher-order polarizabilities have been neglected. FeOCl magnetically orders[27] at about 92 °K. Although there are at least two magnetically nonequivalent sites, the internal magnetic fields H_N as measured at 6 °K are about

the same $H_N \approx 430$ kOe for all sites. This H_N is unusually low for a Fe^{3+} ion and suggests that covalent effects may be important in FeOCl. The value $Q \approx 0.33$ b is considerably larger than recent estimates of $Q \approx 0.20$ b from ferrous quadrupole coupling data[28-33] which, of course, are subject to model-dependent uncertainties also.

It should be possible to observe nuclear quadrupole resonance at the Cl^- site in FeOCl. This additional information would provide valuable checks on the calculation, and conversely, might suggest improvements in the model. The calculations summarized in Table III (including both monopole and dipole contributions) predict a Cl^{35} quadrupole resonance frequency of ≈ 25 MHz for $\alpha_O = \alpha_{Cl} = 1$ Å^3.

Finally, the value of having a nonaxially symmetric EFG as the basis for a quadrupole-moment evaluation is evident if we use only the point-charge contribution in the Q evaluation [Eq. (1)]. This evaluation leads to a Q of 0.20 b in good agreement with currently proposed values based on ferrous quadrupole coupling data. Considering that the experimental and calculated V_{bb} and V_{cc} are interchanged, this agreement is clearly fortuitous.

ACKNOWLEDGMENTS

We thank A. H. Muir, Jr., M. D. Lind, S. Geller, R. G. Wheeler, and W. N. Hardy for helpful discussions. The technical assistance of K. G. Rasmussen and M. R. Bloombaum is appreciated.

APPENDIX

Our previous discussions of dispersion effects (on Mössbauer absorption by single-crystal absorbers) indicated that dispersion had no effect on transmitted intensities in any direction for a two-line quadrupole-split absorber with only one absorbing nucleus per unit cell.[17,34] Actually, the condition requiring only one resonant nucleus per unit cell is too restrictive. It will be shown below that dispersion does not affect the transmitted intensities for any two-line quadrupole-split absorber with an arbitrary number of crystallographically equivalent absorbing nuclei per unit cell even if the principal axes of the EFG tensors at the crystallographically equivalent sites have different orientations with respect to the crystal axes.

Using the notation of Ref. 17, Eq. (11), we may write the contribution to the index of refraction from resonant processes as

$$n_r = \frac{\sigma_o}{2k} \sum_{ij} N_j f_j'(\vec{k}) \begin{pmatrix} \rho_{11}^{ij} & \rho_{12}^{ij} \\ \rho_{21}^{ij} & \rho_{22}^{ij} \end{pmatrix} \left[\frac{(-1)^{1/2} - (x - x_{ij})}{(x - x_{ij})^2 + 1} \right], \tag{A1}$$

where resonant frequencies are identified by subscript i's and resonant sites by j's. Unique sets of resonant sites j are defined as subsets of crystallographically equivalent sites which have identical orientations with respect to $\vec{k}$ (i.e., those related only by simple translational elements of the space group). Quantities not previously defined are N_j, the number of nuclei of type j per unit volume; $f_j'(\vec{k})$, the Debye-Waller factor of site j in the direction $\vec{k}$; and x is a dimensionless energy $x = 2E/\Gamma$ where E is energy.

The polarization dependence of n_r is determined by the density matrices, the elements of which satisfy the relationships

$$\sum_i \rho_{12}^{ij} = \sum_i \rho_{21}^{ij} = 0; \quad \sum_i \rho_{11}^{ij} = \sum_i \rho_{22}^{ij} = 1 . \tag{A2}$$

It is assumed that all density matrices are expressed in terms of the same basis polarizations which can always be achieved by unitary transformations. Because all resonant sites are crystallographically equivalent, N_j and the x_{ij} are equal for all j values; we therefore replace N_j by N. With the definition

$$D_{ij} \equiv D_i = \left[\frac{(-1)^{1/2} - (x - x_{ij})}{(x - x_{ij})^2 + 1} \right] ,$$

the index of refraction for a two-line quadrupole-split doublet is

$$n_r = \frac{\sigma_o N}{2k} \left[D_1 \sum_j f_j'(\vec{k}) \begin{pmatrix} \rho_{11}^{1j} & \rho_{12}^{1j} \\ \rho_{21}^{1j} & \rho_{22}^{1j} \end{pmatrix} + D_2 \sum_j f_j'(\vec{k}) \begin{pmatrix} \rho_{11}^{2j} & \rho_{12}^{2j} \\ \rho_{21}^{2j} & \rho_{22}^{2j} \end{pmatrix} \right] .$$

A unitary transformation exists which will diagonalize the $i = 1$ density matrix. It may be written in simple form using the definition

$$\begin{pmatrix} \rho_{11}^{1} & \rho_{12}^{1} \\ \rho_{21}^{1} & \rho_{22}^{1} \end{pmatrix} = \sum_j f_j'(\vec{k}) \begin{pmatrix} \rho_{11}^{1j} & \rho_{12}^{1j} \\ \rho_{21}^{1j} & \rho_{22}^{1j} \end{pmatrix} .$$

Because of conditions (A2),

$$\begin{pmatrix} \rho_{11}^{2} & \rho_{12}^{2} \\ \rho_{21}^{2} & \rho_{22}^{2} \end{pmatrix} = \begin{pmatrix} 1 & 0 \\ 0 & 1 \end{pmatrix} - \begin{pmatrix} \rho_{11}^{1} & \rho_{12}^{1} \\ \rho_{21}^{1} & \rho_{22}^{1} \end{pmatrix} .$$

Hence, the $i = 2$ density matrix is diagonal in the same system. Therefore, n_r is diagonalizable and dispersion has no effect on absorption.

[1] J. O. Artman, A. H. Muir, Jr., and H. Wiedersich, Phys. Rev. 173, 337 (1968).
[2] J. O. Artman, Phys. Rev. 143, 541 (1966).
[3] R. R. Sharma and T. P. Das, J. Chem. Phys. 41, 3581 (1964).
[4] T. T. Taylor and T. P. Das, Phys. Rev. 133, A1327 (1964).
[5] L. D. V. Rao and D. V. G. L. N. Rao, Phys. Rev. 160, 274 (1967).
[6] M. Raymond and S. S. Hafner, Phys. Rev. B 1, 979 (1970).
[7] D. R. Taylor, J. Chem. Phys. 48, 536 (1968).
[8] G. A. Sawatzky and Julieke Hupkes, Phys. Rev. Letters 25, 100 (1970); G. A. Sawatzky, F. van der Woude,

and Julieke Hupkes (unpublished).
[9]P. A. Flinn (private communication).
[10]R. W. Grant, R. M. Housley, and U. Gonser, Phys. Rev. 178, 523 (1969).
[11]S. Goldsztaub, Bull. Soc. Franc. Mineral 58, 6 (1935).
[12]R. M. Housley, N. E. Erickson, and J. G. Dash, Nucl. Instr. Methods 27, 29 (1964). An additional small background correction of about 2% was made to account for Compton scattering from a Lucite source holder. This correction could be estimated only approximately which increased the uncertainty in the absolute areas but had a negligible effect on the absorption-area ratios.
[13]S. Goldsztaub, Compt. Rend. 198, 667 (1934).
[14]M. D. Lind, Acta Cryst. B26, 1058 (1970).
[15]Throughout this paper a descriptive notation is used, namely, that the "direction" of V_{zz} implies the direction of the z principal axis of the diagonalized EFG, etc.
[16]Unless stated otherwise, the quoted error represents 1 standard deviation of the mean value based on the 22 independent measurements.
[17]R. M. Housley, R. W. Grant, and U. Gonser, Phys. Rev. 178, 514 (1969).
[18]R. M. Housley, J. G. Dash, and R. H. Nussbaum, Phys. Rev. 136, A464 (1964); the effective f of our source was reduced by $\approx 1\%$ because of resonant self-absorption.
[19]A. H. Muir, Jr., K. J. Ando, and H. M. Coogan, *Mössbauer Effect Data Index* 1958-1965 (Interscience, New York, 1966).
[20]U. Gonser and R. W. Grant, Phys. Status Solidi 21, 331 (1967).
[21]C. E. Johnson, W. Marshall, and G. J. Perlow, Phys. Rev. 126, 1503 (1962).
[22]U. Gonser, R. W. Grant, H. Wiedersich, and S. Geller, Appl. Phys. Letters 9, 18 (1966).
[23]W. Rubinson and K. P. Gopinathan, Phys. Rev. 170, 969 (1968).
[24]D. P. Johnson, Phys. Rev. B 1, 3551 (1970).
[25]D. Sengupta and J. O. Artman, Phys. Rev. B 1, 2986 (1970); J. O. Artman, F. deS. Barros, J. Stampfel, J. Viccaro, and R. A. Heinz, Bull. Am. Phys. Soc. 13, 691 (1968); J. O. Artman and J. C. Murphy, Phys. Rev. 135, A1622 (1964).
[26]R. M. Sternheimer, Phys. Rev. 130, 1423 (1963).
[27]R. W. Grant, J. Appl. Phys. (to be published).
[28]R. Ingalls, Phys. Rev. 188, 1045 (1969).
[29]A. J. Nozik, and M. Kaplan, Phys. Rev. 159, 273 (1967).
[30]C. E. Johnson, Proc. Phys. Soc. (London) 92, 748 (1967).
[31]J. Chappert, R. B. Frankel, A. Misetich, and N. A. Blum, Phys. Letters 28B, 406 (1969); Phys. Rev. 179, 578 (1969).
[32]H. R. Leider and D. N. Pipkorn, Phys. Rev. 165, 494 (1968).
[33]F. S. Ham, Phys. Rev. 160, 328 (1967).
[34]R. M. Housley and U. Gonser, Phys. Rev. 171, 480 (1968).

PHYSICAL REVIEW B VOLUME 3, NUMBER 3 1 FEBRUARY 1971

Time-Reversal Experiments in Dipolar-Coupled Spin Systems*

W-K. Rhim, A. Pines, and J. S. Waugh
Department of Chemistry and Research Laboratory of Electronics, Massachusetts Institute of Technology, Cambridge, Massachusetts 02139
(Received 3 September 1970)

By applying a suitable sequence of strong rf fields, a system of dipolar-coupled nuclear spins can be made to behave as though the sign of the dipolar Hamiltonian had been reversed. The system then appears to develop backward in time, and states of nonequilibrium magnetization can be recovered in systems which would superficially appear to have decayed to equilibrium. This behavior is consistent with dynamical and thermodynamical principles, but shows that the spin-temperature hypothesis must be employed with caution. The theory of the time-reversal phenomenon is discussed, including the practical limitations on the accuracy with which it can be achieved. Various echo experiments in the laboratory and in the rotating frame are reported. The application of repeated time reversals to the problem of high-resolution NMR in solids is discussed.

I. INTRODUCTION

One's first impression on seeing a spin echo tends to be of having witnessed a spontaneous fluctuation of an apparently disordered system into an ordered (magnetized) state. Actually, of course, the system was by no means as disordered as it seemed to be: It had to be prepared from a magnetized state in a special way, such that its microscopic dynamical equations guaranteed a return to the magnetized state; and the name "echo" of course expresses just this fact. The importance of a dynamical, as opposed to thermodynamical, interpretation is particularly transparent in the case of the Hahn echo.[1-3] There the spin Hamiltonian is *inhomogeneous*, i.e., it represents a sum over uncoupled spins or isochromats interacting with fixed local fields. One is not dealing with a "many-body" system at all, and the formation of an echo is easily understood by superposing the quantum-